

CONFIDENTIAL

Copy
RM L52E02

NACA RM L52E02

~~FOR~~
NACA
~~NOT TO BE~~

RESEARCH MEMORANDUM

LONGITUDINAL FREQUENCY-RESPONSE AND STABILITY
CHARACTERISTICS OF THE DOUGLAS D-558-II
AIRPLANE AS DETERMINED FROM TRANSIENT
RESPONSE TO A MACH NUMBER OF 0.96

By Euclid C. Holleman

Langley Aeronautical Laboratory
Langley Field, Va.

CLASSIFICATION CHANGED

To **UNCLASSIFIED**

CLASSIFIED DOCUMENT

By authority of *46-115*

Effective
Date *5-8-57*

This material contains information affecting the National Defense of the United States within the meaning of the espionage laws, Title 18, U.S.C., Secs. 793 and 794, the transmission or revelation of which in any manner to unauthorized person is prohibited by law.

at 5-23-57

NATIONAL ADVISORY COMMITTEE FOR AERONAUTICS

WASHINGTON

September 18, 1952

CONFIDENTIAL



NATIONAL ADVISORY COMMITTEE FOR AERONAUTICS

RESEARCH MEMORANDUM

LONGITUDINAL FREQUENCY-RESPONSE AND STABILITY

CHARACTERISTICS OF THE DOUGLAS D-558-II

AIRPLANE AS DETERMINED FROM TRANSIENT

RESPONSE TO A MACH NUMBER OF 0.96

By Euclid C. Holleman

SUMMARY


The longitudinal frequency-response characteristics and the stability derivatives of the Douglas D-558-II airplane were computed from transient-flight data over a Mach number range of 0.60 to 0.96 and at altitude ranges of 21,000 to 25,000 feet, 28,000 to 33,000 feet, and at 37,500 and 43,000 feet. The results are presented as amplitude ratio and phase angle plotted against frequency, and as stability derivatives plotted against Mach number. The response amplitude of the system varied little with Mach number for the Mach number range of these tests; however, the resonant frequency increased with Mach number.

The airplane transfer-function coefficients showed some variation with Mach number and some altitude effects.

The longitudinal-stability derivatives agreed favorably with wind-tunnel results. The elevator control effectiveness varied little with Mach number at the lower Mach numbers but a loss in effectiveness was indicated at the higher test Mach numbers. The static stability of the airplane increased with Mach number for the Mach number range tested. The rate of change of airplane normal-force coefficient with angle of attack increased with Mach number to a Mach number of 0.83. The damping derivative increased with Mach number to a Mach number of about 0.85 and a decrease was indicated to the higher test Mach numbers.

INTRODUCTION

An investigation is currently being conducted by the National Advisory Committee for Aeronautics to determine the dynamic response



characteristics of research airplanes through the transonic speed range. As a part of this investigation, some results on the dynamic longitudinal response characteristics of the Douglas D-558-II research airplane have been obtained. These data are somewhat complete below a Mach number of 0.85 for two altitude ranges. Some data are presented for higher test Mach numbers and altitudes because of the general interest in data of this type.

Of the several methods of obtaining the frequency response of free-flight dynamical systems, the pulse-disturbance technique was used because a minimum of flight time and instrumentation is required. Also, no special device is necessary to actuate the input control. By a Fourier analysis of the airplane response to an elevator pulse, the frequency response of the airplane has been obtained. These results have been reduced to airplane stability derivatives.

These tests were conducted over a Mach number range of 0.60 to 0.96 at altitudes ranging from 21,000 to 43,000 feet. For purposes of analysis the data have been divided into three altitude ranges: 21,000 to 25,000 feet, 28,000 to 33,000 feet, and at 37,500 and 43,000 feet.

SYMBOLS

C_N	airplane normal-force coefficient
α	angle of attack, deg
δ	elevator position, deg or radians
i_t	stabilizer position, deg (positive when airplane nose down)
q	pitching velocity, radians/sec
V	forward velocity, ft/sec
\bar{c}	mean aerodynamic chord, ft
m	mass of the airplane, slugs
S	wing area, sq ft
n	normal acceleration, g units
g	acceleration due to gravity, ft/sec ²

ρ	air density, slugs/cu ft
t	time, sec
T	time to reach steady state, sec
W	airplane weight, lb
h_p	pressure altitude, ft
M	Mach number
I_y	moment of inertia about Y-axis, slug-ft ²
ω	exciting frequency, radians/sec
ω_n	undamped natural frequency of the airplane, radians/sec
ϕ	phase angle between q and δ , deg
C_0, C_1	disturbance function parameters of the transfer function
D	differential operator, d/dt , per sec
ζ	damping ratio, percent damping
C_{L_α}	rate of change of lift coefficient with angle of attack, per deg
C_{L_δ}	rate of change of lift coefficient with elevator deflection, per deg
C_{N_α}	rate of change of airplane normal-force coefficient with angle of attack, per deg
C_{m_α}	rate of change of pitching-moment coefficient with angle of attack, per deg
C_{m_δ}	rate of change of pitching-moment coefficient with elevator deflection, per deg
C_{m_q}	rate of change of pitching-moment coefficient with pitching velocity, per radian
$C_{m_{\dot{\alpha}}}$	rate of change of pitching-moment coefficient with angular velocity of angle of attack, per radian

$C_{mq} + C_{m\dot{\alpha}}$	damping derivative, per deg
R_q, I_q	real and imaginary parts of the output function, respectively
R_δ, I_δ	real and imaginary parts of the input function, respectively
q_R, q_I	transient real and imaginary parts of the output function (evaluated to time T), respectively
δ_R, δ_I	transient real and imaginary parts of the input function (evaluated to time T), respectively

$$\dot{\alpha} = \frac{d\alpha}{dt}$$

$$\dot{q} = \frac{dq}{dt}$$

$$Z_\alpha = -\frac{1}{2}\rho V^2 S C_{L\alpha}$$

$$Z_\delta = \frac{1}{2}\rho V^2 S C_{L\delta}$$

$$M_\alpha = \frac{1}{2}\rho V^2 S \bar{c} C_{m\alpha}$$

$$M_{\dot{\alpha}} = \frac{1}{4}\rho V S \bar{c}^2 C_{m\dot{\alpha}}$$

$$M_q = \frac{1}{4}\rho V S \bar{c}^2 C_{mq}$$

$$M_\delta = \frac{1}{2}\rho V^2 S \bar{c} C_{m\delta}$$

TEST EQUIPMENT

Airplane

The test airplane, the Douglas D-558-II, is a midwing research airplane with swept-wing and tail surfaces. It is both jet and rocket powered. The jet engine exhausts out the bottom of the fuselage between

the wing and tail at an angle of approximately 8° to the center line of the airplane fuselage with the thrust line approximately through the airplane center of gravity. The rocket engine exhausts out the rear of the fuselage with the thrust line along the fuselage center line. Below a Mach number of 0.85 the aircraft was jet powered only. The airplane was maneuvered by conventional controls and trimmed longitudinally by a movable stabilizer. For most of the test maneuvers, the stabilizer was fixed at 2.1° , trailing edge down. Presented in figure 1 is a three-view drawing of the airplane and table I gives the physical characteristics of the airplane.

The moment of inertia of the airplane was determined experimentally by the method outlined in reference 1 and was corrected analytically for changes in weight due to fuel consumption. Airplane weights, moments of inertia, and center-of-gravity locations are presented in table I.

Instrumentation

The test airplane was completely instrumented for an extensive flight-test program of which the tests reported herein were a part. Standard recording NACA instruments were used and were synchronized by a common timer. Quantities measured pertinent to the investigation are as follows: airspeed, altitude, normal acceleration, pitching velocity, elevator position, stabilizer position, angle of attack, and fuel remaining.

Other recorded quantities, such as rolling and yawing velocity, pitching acceleration, transverse and longitudinal acceleration, and aileron and rudder position, were available for a complete evaluation of the maneuver.

The recording pitch turnmeter was located as near as possible to the airplane center of gravity and had a range of ± 1 radian per second. The instrument used was a direct-recording-rate gyro with a natural frequency of 14 cycles per second and a damping ratio of 0.65 critical. The elevator position was recorded with an external control-position transmitter (C.P.T.) and recorder and was measured referenced to the stabilizer. The stabilizer position was measured referenced to the airplane center line.

Accuracies of the recorded data are indicated by the following instrument accuracies:

Pitching velocity, q , radians/sec	± 0.005
Normal acceleration, n , g units	± 0.025
Mach number, M	± 0.01
Elevator position, δ , deg	± 0.2
Stabilizer position, i_t , deg	± 0.1
Angle of attack, α , deg	± 0.2

The angle of attack was measured by a vane located approximately 25 feet ahead of the center of gravity of the airplane and was not corrected for position error.

METHOD OF OBTAINING DATA

Airplane responses were recorded over a test Mach number range of 0.61 to 0.96 and over an altitude range of from 21,000 to 43,000 feet. Stabilized flight was established before each maneuver to minimize variation in speed and altitude. The test maneuver consisted of disturbing the airplane from stabilized flight by a pulse of the elevator control. Airplane responses were obtained as a result of both up and down pulses of the elevator. For most of the maneuvers, the stabilizer was fixed at approximately the same position of 2.1° , trailing edge down; however, the stabilizer is the only trimming device on the airplane so that for some runs the stabilizer position was slightly different. The elevator pulse was of the order of 5° for about 1-second duration. An attempt was made to return the elevator control to its original position for trim. The resulting airplane response was a normal acceleration of approximately $\pm 1g$ or pitching velocity of ± 0.2 radian per second and was recorded until the airplane oscillation subsided to some steady-state condition. An average of about 7 seconds of flight time was required for one airplane transient response from which an entire frequency response was obtained.

METHOD OF ANALYSIS

The method of analysis is broken down into three distinct phases: determination of the frequency response; calculation of the transfer-function coefficients; determination of the stability derivatives.

Determination of the Frequency Response

Time histories of the airplane pitching-velocity response to a pulse of the elevator provide the working data (figs. 2 and 3). These data were tabulated every 0.05 second which kept the accuracy of the method within 1 percent (ref. 2) and were transformed from the time plane to the frequency plane by a solution of the Fourier integrals,

$$q(\omega) = \int_0^{\infty} q(t)e^{-i\omega t} dt \quad (1)$$

$$\delta(\omega) = \int_0^{\infty} \delta(t)e^{-i\omega t} dt \quad (2)$$

as was done in references 2 and 3. These integrals were evaluated in two parts - the transient and the steady state. The transient integrals were evaluated by numerical integration (Simpson's one-third-rule integration). For this analysis, integrations were made at frequencies of 45, 60, 90, 120, 180, 225, 300, and 360 degrees per second.

Once the complete Fourier integrals R_q , I_q , R_δ , and I_δ are evaluated, they may be combined to give the frequency response

$$\frac{q}{\delta} = \left| \frac{q}{\delta} \right| e^{i\phi} \quad \text{in terms of amplitude ratio}$$

$$\left| \frac{q}{\delta} \right| = \frac{\sqrt{R_q^2 + I_q^2}}{\sqrt{R_\delta^2 + I_\delta^2}} \quad (3)$$

and phase angle

$$\phi = \tan^{-1} \frac{I_q}{R_q} - \tan^{-1} \frac{I_\delta}{R_\delta} \quad (4)$$

Calculation of the Transfer-Function Coefficients

For this analysis it is assumed that a two-degree-of-freedom system adequately describes the airplane longitudinally. Equations of motion for such a system are, as reported in reference 2,

$$mV(\dot{\alpha} - q) = Z_\alpha \alpha + Z_\delta \delta \quad (5)$$

$$I_y \dot{q} = M_q q + M_\alpha \alpha + M_{\dot{\alpha}} \dot{\alpha} + M_\delta \delta \quad (6)$$

The transfer-function equation of the system as obtained by solving the equations of motion simultaneously is

$$D^2q + 2\zeta\omega_n Dq + \omega_n^2 q = C_0\delta + C_1 D\delta \quad (7)$$

where the transfer-function coefficients C_0 , C_1 , $2\zeta\omega_n$, and $(\omega_n)^2$ are

$$C_1 = \frac{\frac{1}{2}\rho V^2 S \bar{c}}{I_y} \left(\frac{\frac{1}{4}\rho S \bar{c} C_{L\delta} C_{m\dot{\alpha}}}{m} + C_{m\delta} \right) \quad (8)$$

$$C_0 = \frac{\rho^2 V^3 S^2 \bar{c}}{4 I_y m} (C_{L\delta} C_{m\alpha} + C_{L\alpha} C_{m\delta}) \quad (9)$$

$$2\zeta\omega_n = \frac{1}{2}\rho V S \left[\frac{C_{L\alpha}}{m} - \frac{\bar{c}^2}{2 I_y} (C_{mq} + C_{m\dot{\alpha}}) \right] \quad (10)$$

$$(\omega_n)^2 = \frac{\frac{1}{2}\rho V^2 S \bar{c}}{I_y} \left(\frac{\frac{1}{4}\rho S \bar{c}}{m} C_{L\alpha} C_{mq} + C_{m\alpha} \right) \quad (11)$$

By applying the Fourier transform to equation (7) (ref. 4), a real and an imaginary equation in the incomplete Fourier integrals of the input and output functions and the imposed exciting frequencies are obtained:

Real equation

$$\begin{aligned} q_R(\omega_n)^2 + (q_T \cos \omega T - q_I \omega) 2\zeta\omega_n - \delta_R C_0 + \\ (\delta_I \omega - \delta_T \cos \omega T) C_1 = q_R \omega^2 - \omega q_T \sin \omega T \end{aligned} \quad (12)$$

Imaginary equation

$$\begin{aligned} q_I(\omega_n)^2 + (\omega q_R - q_T \sin \omega T) 2\zeta\omega_n - \delta_I C_0 + \\ (\delta_T \sin \omega T - \omega \delta_R) C_1 = q_I \omega^2 - \omega q_T \cos \omega T \end{aligned} \quad (13)$$

By substitution of the incomplete Fourier integrals q_R , q_I , δ_R , and δ_I , the final steady-state values of q_T and δ_T , and the exciting frequencies into equations (12) and (13), a real and an imaginary equation in the four transfer-function coefficients C_0 , C_1 , $2\zeta\omega_n$, and $(\omega_n)^2$ are obtained. Thus, the 8 frequencies yield 16 equations in the 4 unknowns and a solution may be obtained by a least-squares and matrix solution (ref. 4).

As reported in reference 2, film reading appears to be the largest source of error in the reduction of the data. As the test points indicate in figures 4 to 6, the error is more pronounced at the higher frequencies. In the further reduction of these data, a least-squares solution is used. This method weights each frequency evenly; therefore, errors at the higher frequencies give rise to errors in the transfer-function coefficients which subsequently appear in the stability derivatives.

Determination of the Stability Derivatives

The stability derivatives for the airplane may be calculated from equations (8) to (11). A measure of the elevator control effectiveness is obtained from equation (8) as

$$C_{m\delta} = C_{lI_y} \frac{2}{\rho V^2 S \bar{c}} - \frac{\rho S \bar{c}}{4m} C_{L\delta} C_{m\dot{\alpha}} \quad (14)$$

Calculations show the term $-\frac{\rho S \bar{c}}{4m} C_{L\delta} C_{m\dot{\alpha}}$ less than 1 percent of the term $C_{lI_y} \frac{2}{\rho V^2 S \bar{c}}$ so that the equation may be simplified to

$$C_{m\delta} = \frac{2C_{lI_y}}{\rho V^2 S \bar{c}} \quad (15)$$

Equation (11) may be solved to give a measure of the static stability of the airplane as pitching moment due to angle of attack as

$$C_{m\alpha} = -\frac{2I_y(\omega_n)^2}{\rho V^2 S \bar{c}} - \frac{1}{m} \frac{\rho S \bar{c}}{4} C_{L\alpha} C_{m\dot{q}} \quad (16)$$

Calculations also show the term $-\frac{1}{m} \rho S \bar{c} C_{L\alpha} C_{m\dot{\alpha}}$ to be small compared to $-\frac{2I_y(\omega_n)^2}{\rho V^2 \bar{c}}$ so that it may be omitted. The simplified equation is

$$C_{m\alpha} = -\frac{2I_y}{\rho V^2 \bar{c}} (\omega_n)^2 \quad (17)$$

Equation (10) gives a measure of the damping characteristics of the airplane. Solving for the damping derivative gives

$$C_{m\dot{\alpha}} + C_{m\alpha} = \frac{2I_y}{\bar{c}^2} \left[-\frac{2}{\rho V S} (2\zeta \omega_n) + \frac{C_{L\alpha}}{m} \right] \quad (18)$$

The airplane normal-force-coefficient slope was obtained by plotting the airplane normal-force coefficient against the angle of attack measured during the subsidence of the airplane oscillation.

RESULTS AND DISCUSSION

Presented as figures 2(a) and 2(b) are two representative time histories of the airplane response to an elevator pulse. The recorded quantities of pitching velocity and elevator position were analyzed to give the longitudinal frequency response of the system and the longitudinal stability derivatives. Figure 3 shows the trim airplane normal-force coefficient at an airplane weight of 11,000 pounds $\left(\frac{W}{S} = 63 \text{ lb/sq ft}\right)$ as a function of Mach number with the mean normal-force coefficient during each test run shown as the test points. The test points for the two altitude ranges of 21,000 to 25,000 feet and 28,000 to 33,000 feet are shown by the flagged and unflagged circles, respectively. The square and diamond indicate the points at altitudes of 37,500 and 43,000 feet. All tests at the lower Mach numbers were made with jet power only; however, the higher-speed runs necessitated the use of both rocket and jet power. These runs were made at a higher altitude and at a heavier airplane weight and consequently higher C_N .

Frequency Response

The frequency response of the system for the different test conditions of Mach number and altitude is presented in figures 4 to 6 as amplitude ratio and phase angle as a function of exciting frequency. During each run the stabilizer position was constant; however, the stabilizer position varied slightly for some of the test runs as is noted in each figure.

Figures 4(a) to 4(f) present the frequency response of the system for an altitude range of 21,000 to 25,000 feet. These results are presented as amplitude ratio q/δ and phase angle ϕ as a function of frequency ω with the calculated points indicated as circles and squares. Lines are faired and the results are compared for the different Mach numbers in figure 4(g). Figures 5(a) to 5(g) present results obtained at an altitude range of 28,000 to 33,000 feet with the runs compared in figure 5(h). Figures 6(a) and 6(b) present the frequency response at altitudes of 43,000 and 37,500 feet. These tests are for a Mach number of 0.90 and 0.93 and the runs are compared in figure 6(c). For the limited range of these tests little change in amplitude ratio with Mach number is shown; however, a change of about 1 in amplitude ratio from the higher-altitude data to the low-altitude results is shown. The resonant frequency of the system increases with Mach number from about 2 to 4 radians per second.

By assuming that a two-degree-of-freedom system adequately describes the airplane system longitudinally, the transfer-function coefficients C_0 , C_1 , $2\zeta\omega_n$, and $(\omega_n)^2$ were obtained for each of the responses and are presented as functions of Mach number for the test altitude ranges in figure 7. The flagged circles indicate runs grouped at an altitude range of 21,000 to 25,000 feet. A possible fairing of these data is indicated by the dashed lines. The variation of the transfer-function coefficients with Mach number for the altitude range of 28,000 to 33,000 feet is indicated by the circles. The test points at Mach numbers of 0.90 and 0.93 are at a higher test altitude and are indicated as the diamond and square. The disturbance parameters C_0 and C_1 decrease gradually while the damping parameter $2\zeta\omega_n$ and the undamped natural frequency parameter $(\omega_n)^2$ increase with Mach number to a Mach number of 0.85. At a constant Mach number, the damping parameter, disturbance parameter, and the undamped-natural-frequency parameter decrease with increasing altitude.

Longitudinal Stability Derivatives

By the method outlined, the airplane transfer-function coefficients may be reduced to airplane stability derivatives. Plots of the

derivatives $C_{m\delta}$, $C_{m\alpha}$, $C_{N\alpha}$, and $C_{m_q} + C_{m\dot{\alpha}}$ as functions of Mach number are presented as figure 8. Fairings are indicated for the altitude ranges of 21,000 to 25,000 feet and 28,000 to 33,000 feet. The two test points at the higher altitudes are shown by the diamond and square.

Elevator effectiveness.- The elevator control effectiveness $C_{m\delta}$ is presented for the test altitude ranges (fig. 8) and shows little change with Mach number up to a Mach number of about 0.85. A decrease in effectiveness is indicated to the higher test Mach numbers. The lower-altitude data show approximately 50 percent greater effectiveness than the higher-altitude results.

Static stability.- A measure of the airplane static stability was also obtained and is presented as a function of Mach number in figure 8. The static stability $C_{m\alpha}$ increases gradually from -0.01 at a Mach number of 0.61 to -0.017 at a Mach number of 0.85. At the higher Mach numbers it is indicated that the static stability increases more rapidly. The rate of change of airplane normal-force coefficient with angle of attack $C_{N\alpha}$ is shown as a function of Mach number. This variation shows a gradual increase from 0.07 at a Mach number of 0.61 to 0.088 at a Mach number of 0.83 and has a value of 0.071 at a Mach number of 0.96. Because of malfunctioning of the airplane angle-of-attack vane, data were not available over the dashed part of the curve.

Damping derivative.- From the transfer-function coefficient $2\zeta\omega_n$, the damping derivative $C_{m_q} + C_{m\dot{\alpha}}$ is derived and is presented in figure 8 as a function of Mach number for the test altitudes. Fairings are indicated for the data at altitudes of 21,000 to 25,000 feet and 28,000 to 33,000 feet. The points at altitudes of 37,500 and 43,000 feet are indicated as a square and a diamond, respectively. The damping derivatives for the lower-altitude runs, indicated by the dashed line, show greater damping than the higher-altitude data. The value of $C_{m_q} + C_{m\dot{\alpha}}$ for the altitude range of 28,000 to 33,000 feet varied from -0.23 at a Mach number of 0.62 to -0.58 at a Mach number of 0.85. A rapid decrease is indicated to a value of -0.11 at a Mach number of 0.96.

Comparison of Flight-Test and Wind-Tunnel Data

Presented as figure 9 is a comparison of the flight-test data for the two altitude ranges and that derived from wind-tunnel tests (ref. 5). The wind-tunnel results are for sea-level conditions with a center-of-gravity location of 20.2 percent mean aerodynamic chord, whereas the flight data are for an altitude of from 21,000 to 25,000 feet and 28,000 to 33,000 feet and with a center-of-gravity location of 25 to 26 percent mean aerodynamic chord.

Elevator effectiveness.- The elevator effectiveness $C_{m\delta}$ from flight tests at 28,000 to 33,000 feet is lower by about 0.007 than wind-tunnel results (fig. 9). The flight data for the lower altitude are nearer in agreement with the wind-tunnel results, and if the differences in test conditions are considered, the agreement is believed reasonable. Both flight and wind-tunnel tests indicate a rapid loss of control effectiveness at Mach numbers greater than 0.90 and approach the same value at the highest test Mach number.

Static stability.- A comparison of the static stability derivative $C_{m\alpha}$ as measured during the flight tests and as calculated from the wind-tunnel data is presented in figure 9. The static stability derivative measured during flight tests is about 0.005 lower than that obtained during wind-tunnel tests; however, the difference in center-of-gravity location for the tests would indicate a difference of this order of magnitude. Also presented is a comparison between the rate of change of airplane normal-force coefficient with angle of attack $C_{N\alpha}$ (presented as flight tests) and the rate of change of lift coefficient with angle of attack (indicated as wind-tunnel data). Reasonable agreement is obtained over the Mach number range with the flight data slightly higher at the middle Mach number range.

Damping derivative.- Presented also in figure 9 is a comparison of flight-test damping derivative $C_{mq} + C_{m\dot{\alpha}}$ and wind-tunnel values of $C_{mq} + C_{m\dot{\alpha}}$ calculated from wind-tunnel tests by a method from reference 6. The value of $C_{mq} + C_{m\dot{\alpha}}$ from the flight tests for an altitude range of 28,000 to 33,000 feet is lower than the wind-tunnel tests by 0.11 at a Mach number of 0.625; however, the flight data increase to 0.13 greater than wind-tunnel data at a Mach number of 0.85. Thus, the flight-test damping derivative shows a greater variation over the Mach number range than the wind-tunnel tests indicate. The lower-altitude tests indicate greater damping as would be expected. Agreement between these results and wind-tunnel results is considered reasonable.

CONCLUDING REMARKS

By application of the Fourier integral transformation a graphical frequency response of the Douglas D-558-II airplane was obtained from the measured airplane response to pulses of the elevator control.

For the Mach number range of these tests little change in amplitude ratio with Mach number was shown; however, the resonant frequency of the system did increase with Mach number.

The computed transfer-function coefficients showed some variation with Mach number. The disturbance parameters showed an increase negatively with Mach number. The damping transfer-function coefficient and undamped natural frequency parameter increased with Mach number to a Mach number of approximately 0.85.

The longitudinal stability derivatives agreed favorably with wind-tunnel results. The control effectiveness varied little with Mach number to a Mach number of 0.85 and a decrease was indicated to the higher test Mach numbers. The static stability of the airplane increased with Mach number with more rapid increase at the higher Mach numbers. The rate of change of airplane normal-force coefficient with angle of attack increased with Mach number to a Mach number of 0.83 and had a value of 0.071 at a Mach number of 0.96. The damping derivative increased with Mach number to a Mach number of about 0.85 and lower damping was indicated at the higher test Mach numbers.

Langley Aeronautical Laboratory
National Advisory Committee for Aeronautics
Langley Field, Va.

REFERENCES

1. Turner, Howard L.: Measurement of the Moments of Inertia of an Airplane by a Simplified Method. NACA TN 2201, 1950.
2. Triplett, William C., and Smith, G. Allan: Longitudinal Frequency-Response Characteristics of a 35° Swept-Wing Airplane As Determined From Flight Measurements, Including a Method for the Evaluation of Transfer Functions. NACA RM A51G27, 1951.
3. Angle, Ellwyn E., and Holleman, Euclid C.: Longitudinal Frequency-Response Characteristics of the Douglas D-558-I Airplane As Determined From Experimental Transient-Response Histories to a Mach Number of 0.90. NACA RM L51K28, 1952.
4. Greenberg, Harry: A Survey of Methods for Determining Stability Parameters of an Airplane From Dynamic Flight Measurements. NACA TN 2340, 1951.
5. Osborne, Robert S.: High-Speed Wind-Tunnel Investigation of the Longitudinal Stability and Control Characteristics of a $\frac{1}{16}$ -Scale Model of the D-558-2 Research Airplane at High Subsonic Mach Numbers and at a Mach Number of 1.2. NACA RM L9C04, 1949.
6. Greenberg, Harry, and Sternfield, Leonard: A Theoretical Investigation of Longitudinal Stability of Airplanes With Free Controls Including Effect of Friction in Control System. NACA Rep. 791, 1944. (Supersedes NACA ARR 4B01.)

TABLE I

PHYSICAL CHARACTERISTICS OF THE DOUGLAS D-558-II AIRPLANE

Wing:

Root airfoil section (normal to 0.30 chord)	NACA 63-010
Tip airfoil section (normal to 0.30 chord)	NACA 63 ₁ -012
Total area, sq ft	175.0
Span, ft	25.0
Mean aerodynamic chord, ft	7.27
Taper ratio	0.565
Aspect ratio	3.570
Sweep at 0.30 chord, deg	35.0
Incidence at fuselage center line, deg	3.0

Horizontal tail:

Area (including fuselage), sq ft	39.9
Span, in.	143.6
Mean aerodynamic chord, ft	3.48
Taper ratio	0.50
Aspect ratio	3.59
Sweep at 0.30 chord line, deg	40.0
Elevator area, sq ft	9.4
Elevator travel, deg	
Up	25
Down	15

Fuselage:

Length, ft	42.0
Maximum diameter, in.	60.0

Engines:

Turbojet	Westinghouse J-34
Rocket	Reaction Motors

Airplane weight:

Full jet and rocket fuel, lb	15,130
Full jet fuel, lb	11,942
No fuel, lb	10,382

Center-of-gravity locations:

Full jet and rocket fuel (gear up), percent mean aerodynamic chord	23.5
Full jet fuel (gear up), percent mean aerodynamic chord	25.2
No fuel (gear up), percent mean aerodynamic chord	26.5

TABLE I

PHYSICAL CHARACTERISTICS OF THE DOUGLAS D-558-II AIRPLANE - Concluded

Moments of inertia:

Full jet and rocket fuel, slug-ft ²	39,600
Full jet fuel, slug-ft ²	34,600
No fuel, slug-ft ²	33,300

The NACA logo, consisting of the letters "NACA" inside a stylized wing shape.

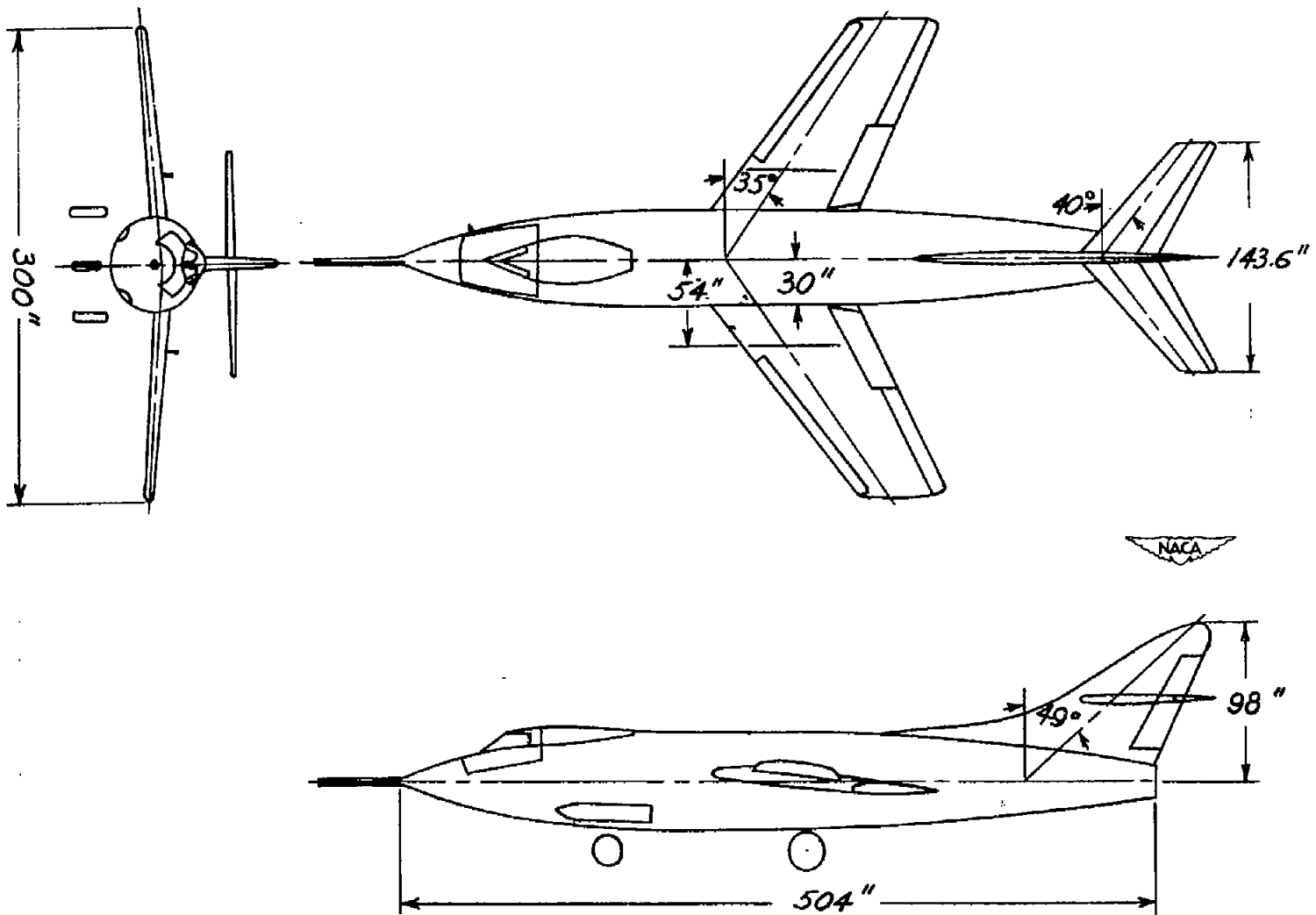
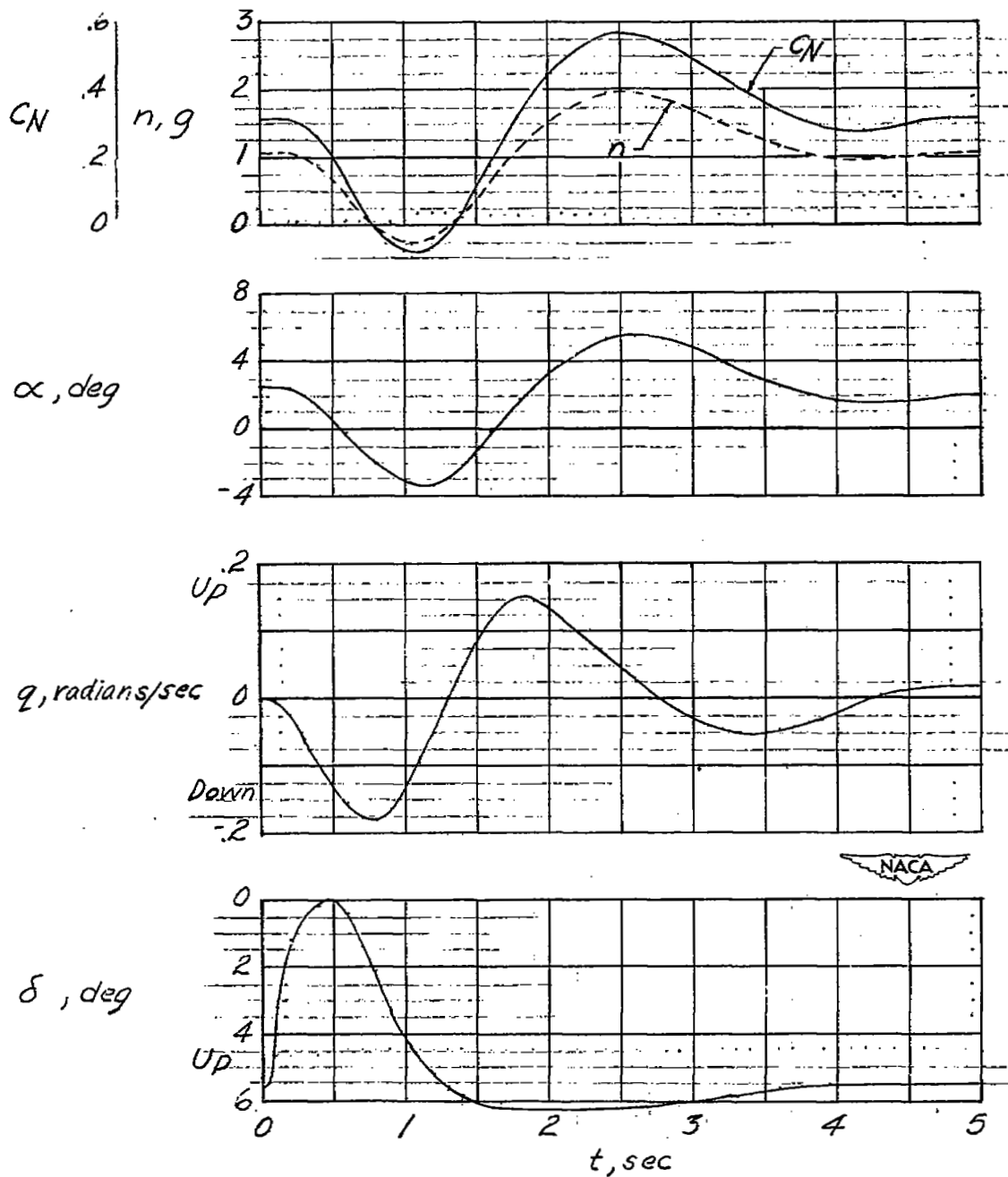
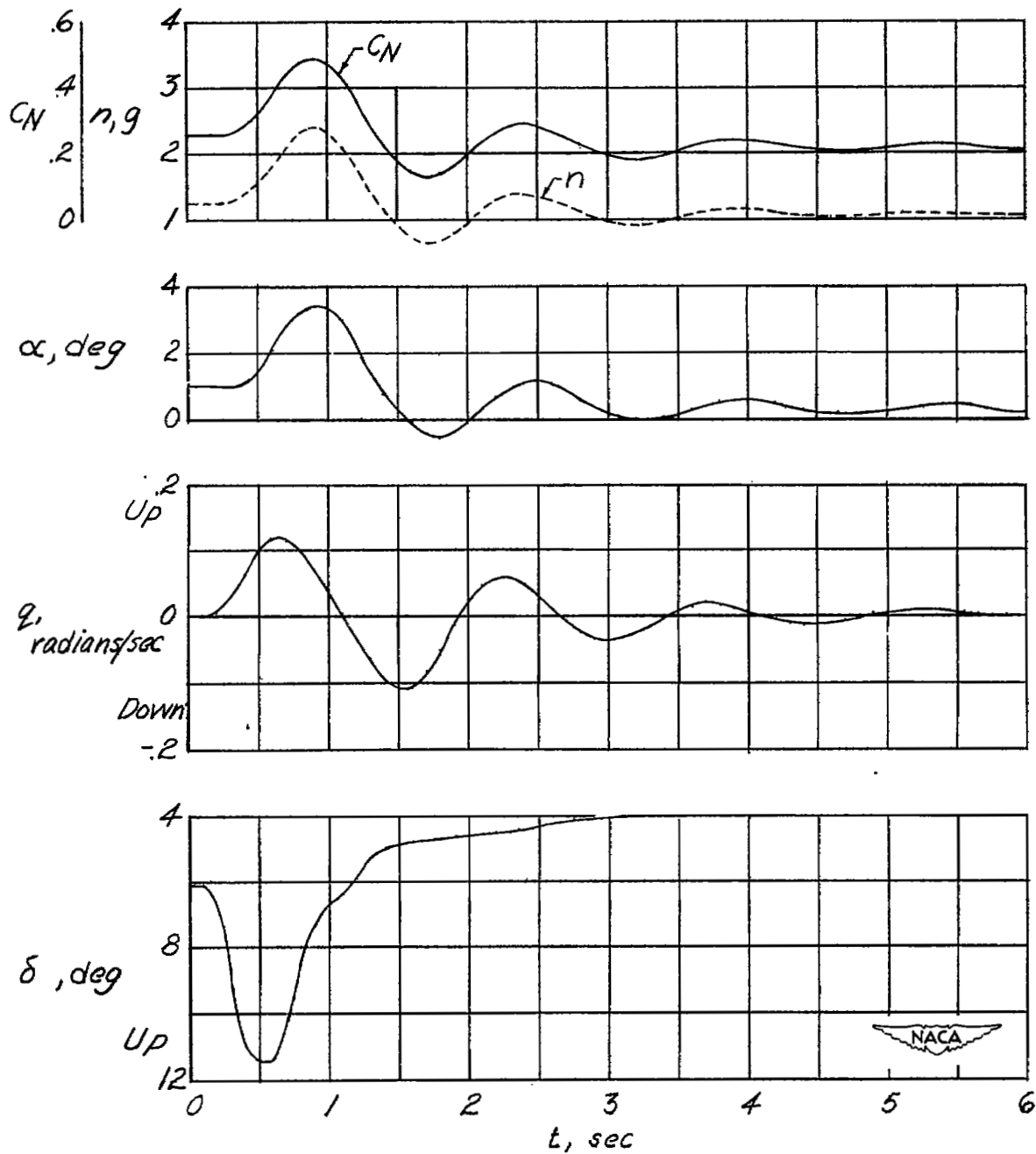


Figure 1.- Three-view drawing of Douglas D-558-II airplane.



(a) $M = 0.64$; $h_p = 25,000$ feet; $i_t = 2.1^\circ$.

Figure 2.- Time history of a typical airplane response to an elevator pulse.



(b) $M = 0.96$; $h_p = 33,000$ feet; $i_t = 1.6^\circ$.

Figure 2.- Concluded.

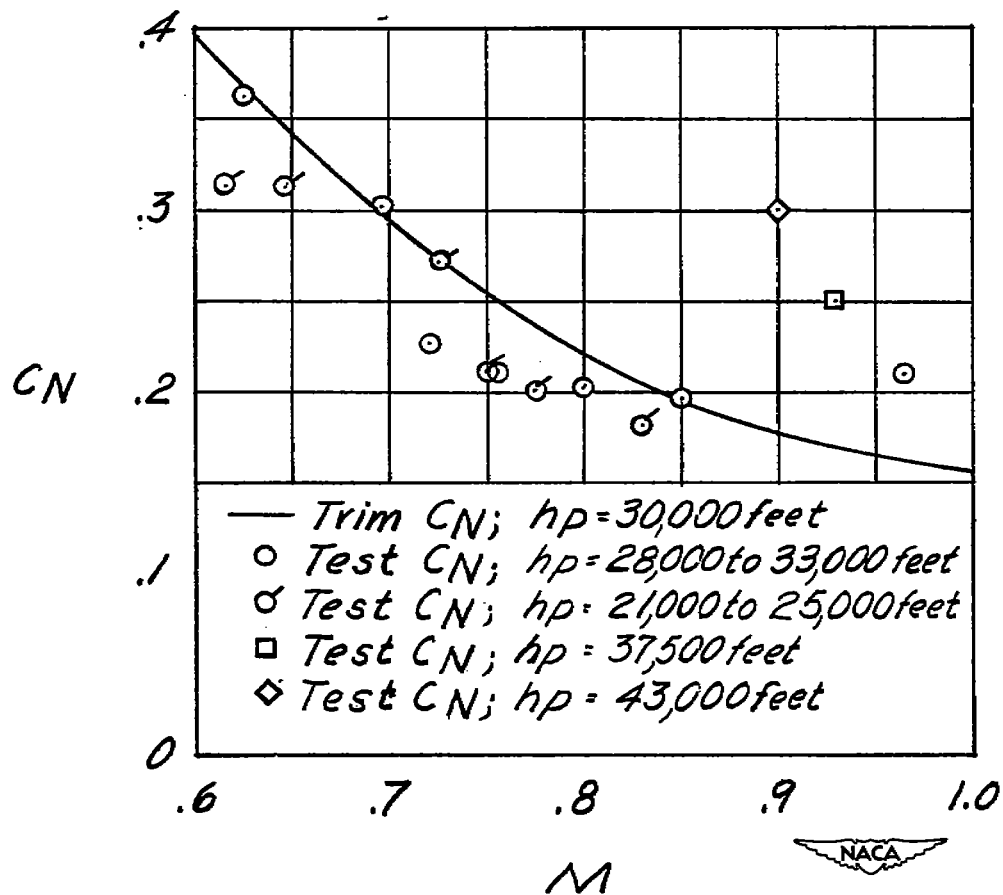
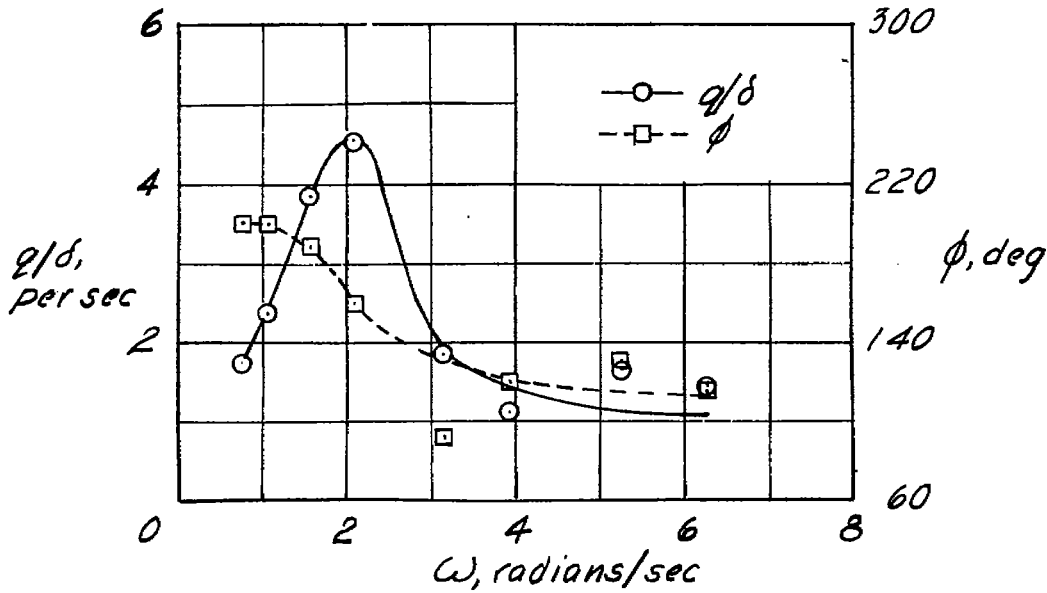
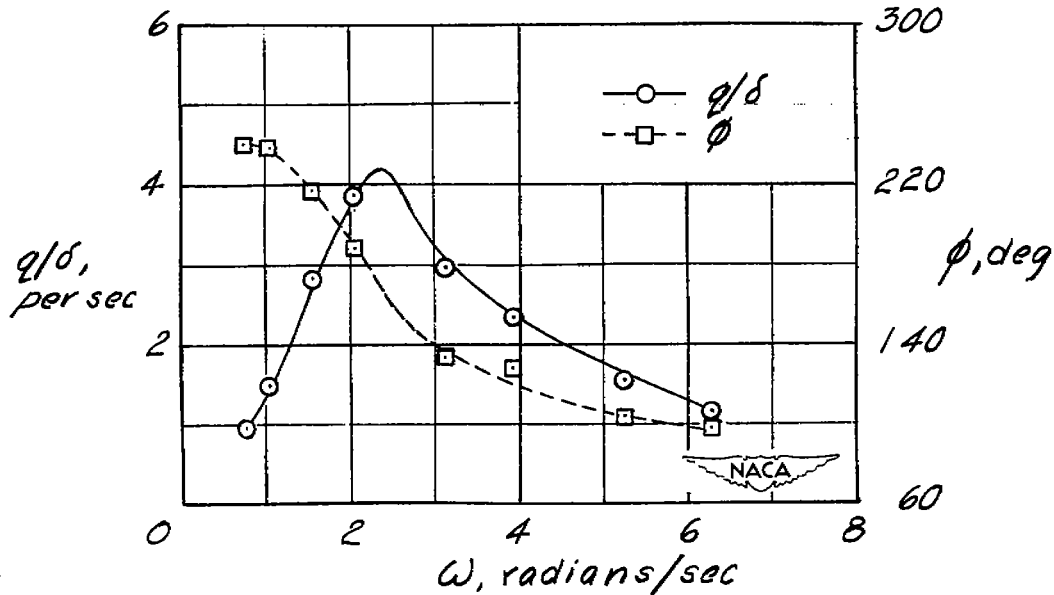


Figure 3.- Variation of the mean normal-force coefficient with Mach number during the test maneuver as compared with the trim normal-force coefficient for the airplane at 30,000 feet with a wing loading of 63 pounds per square foot.

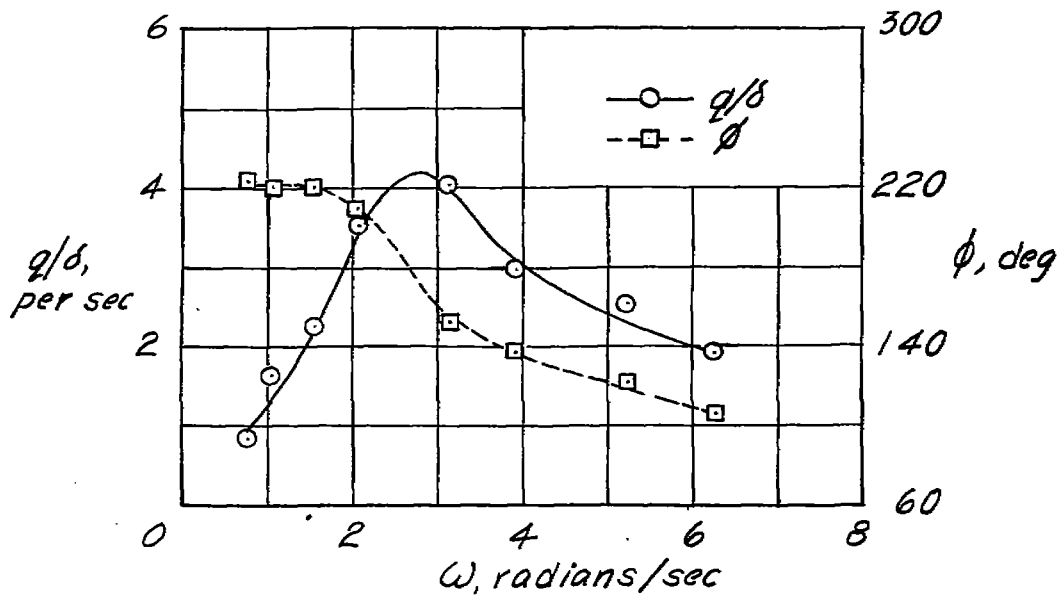


(a) $M = 0.61$; $h_p = 25,000$ feet; $i_t = 2.1^\circ$.

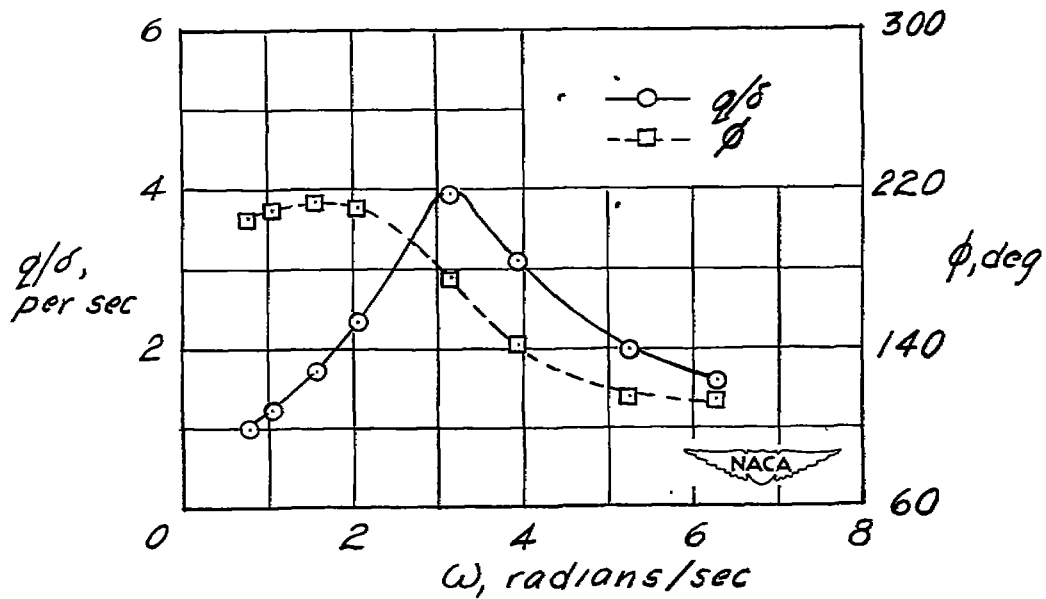


(b) $M = 0.64$; $h_p = 25,000$ feet; $i_t = 2.1^\circ$.

Figure 4.- Frequency response of the Douglas D-558-II airplane as determined from the pitching velocity response to an elevator pulse. $h_p = 21,000$ to $25,000$ feet.

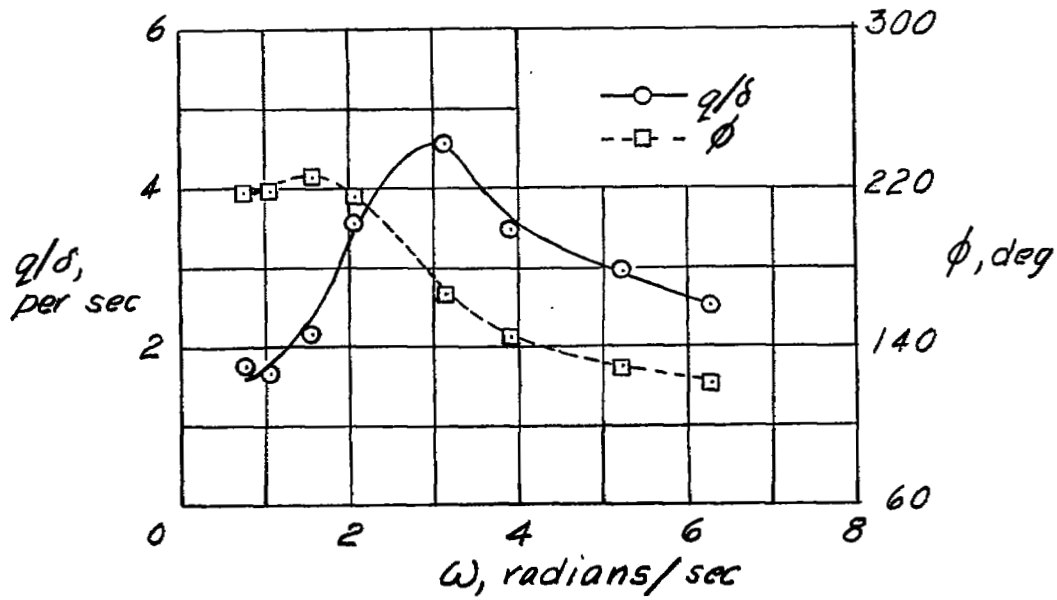


(c) $M = 0.72$; $h_p = 24,000$ feet; $i_t = 2.1^\circ$.

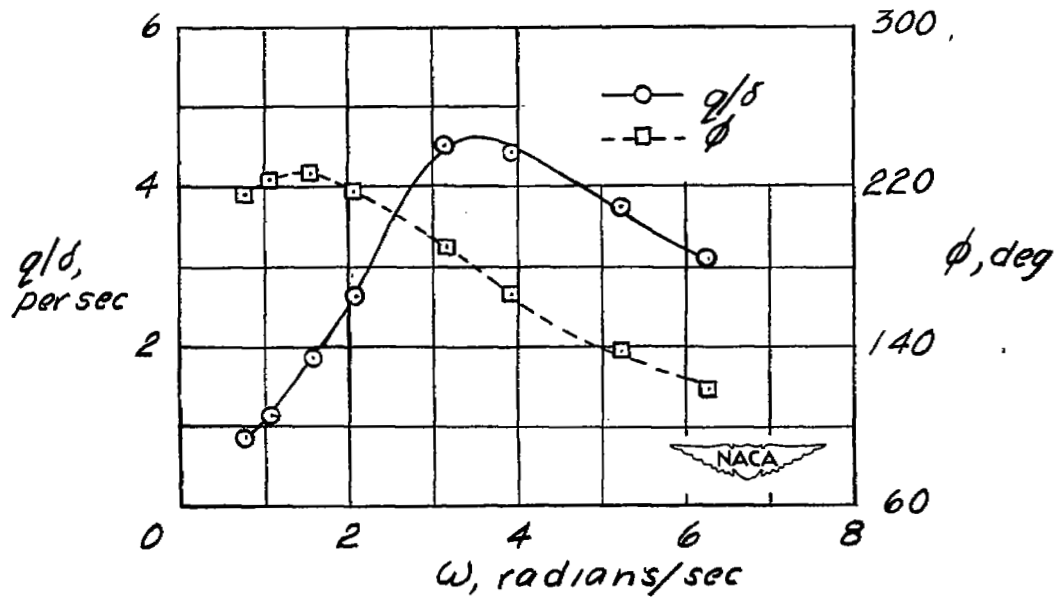


(d) $M = 0.75$; $h_p = 21,000$ feet; $i_t = 0.9^\circ$.

Figure 4.- Continued.

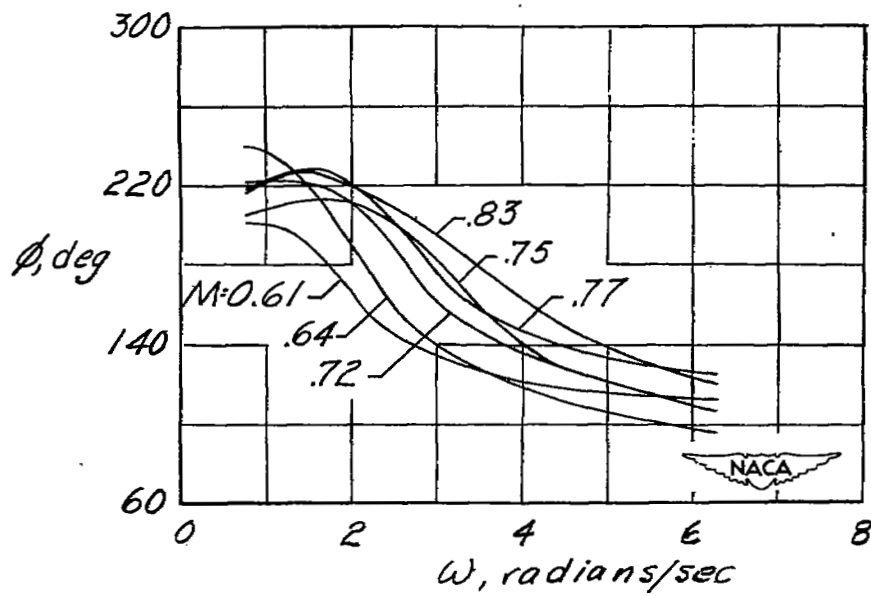
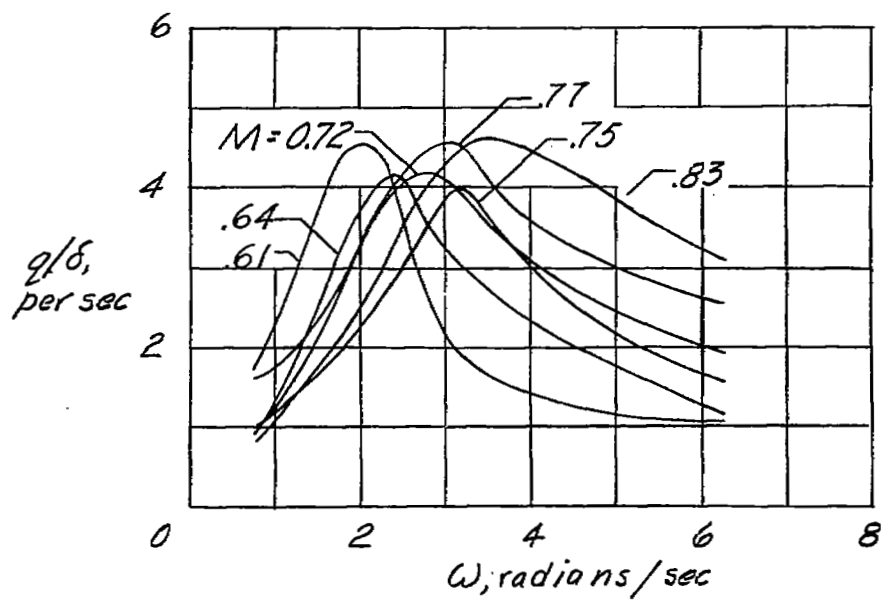


(e) $M = 0.77$; $h_p = 23,000$ feet; $i_t = 2.1^\circ$.



(f) $M = 0.83$; $h_p = 21,000$ feet; $i_t = 2.4^\circ$.

Figure 4.- Continued.



(g) $h_p = 21,000$ to $25,000$ feet.

Figure 4.- Concluded.

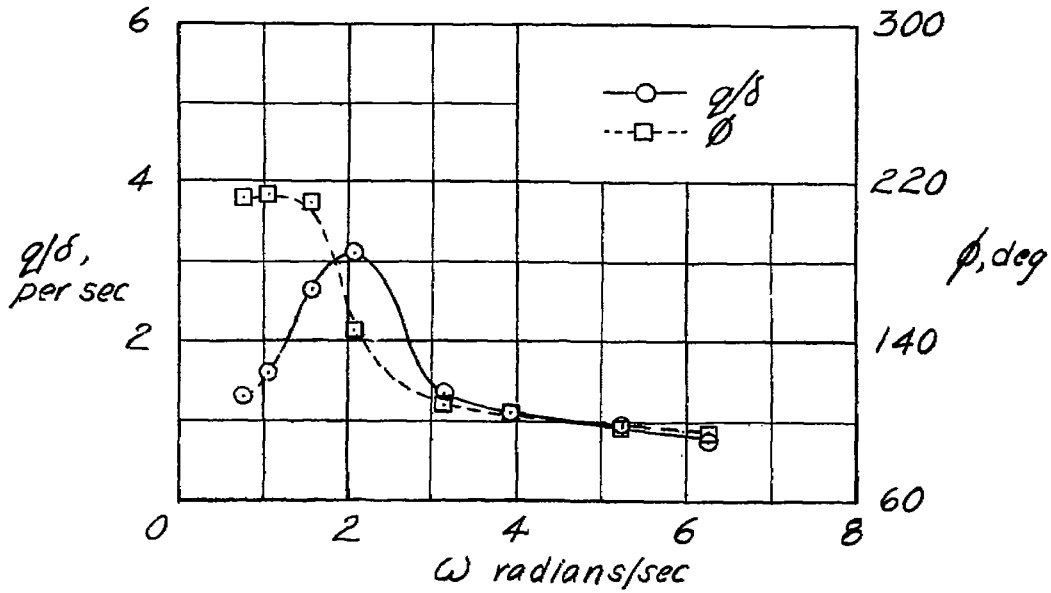
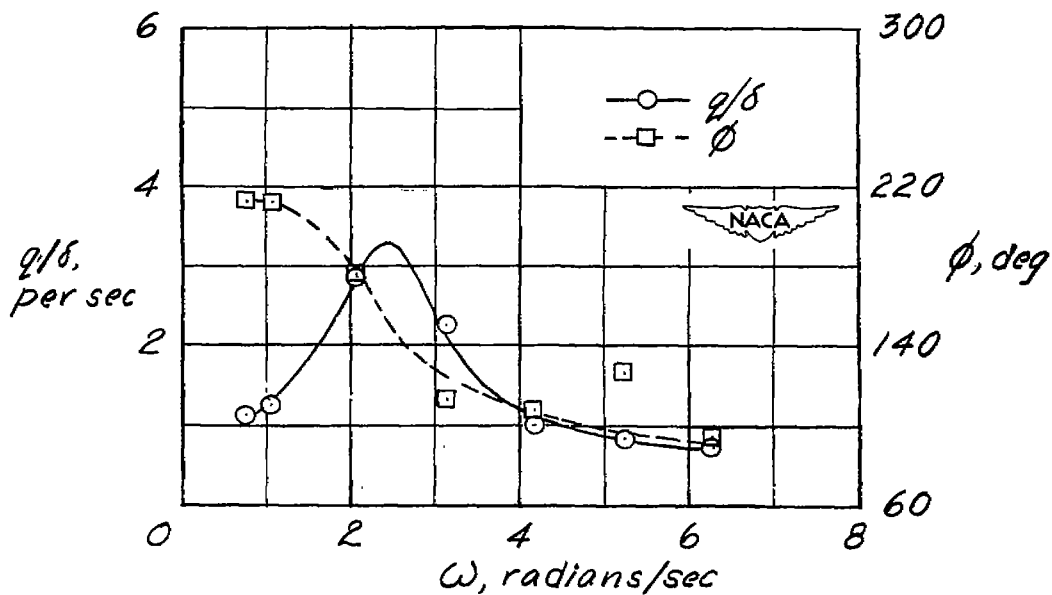
(a) $M = 0.62$; $h_p = 32,000$ feet; $i_t = 2.1^\circ$.(b) $M = 0.70$; $h_p = 31,000$ feet; $i_t = 2.1^\circ$.

Figure 5.- Frequency response of the Douglas D-558-II airplane for an altitude range of 28,000 to 33,000 feet.

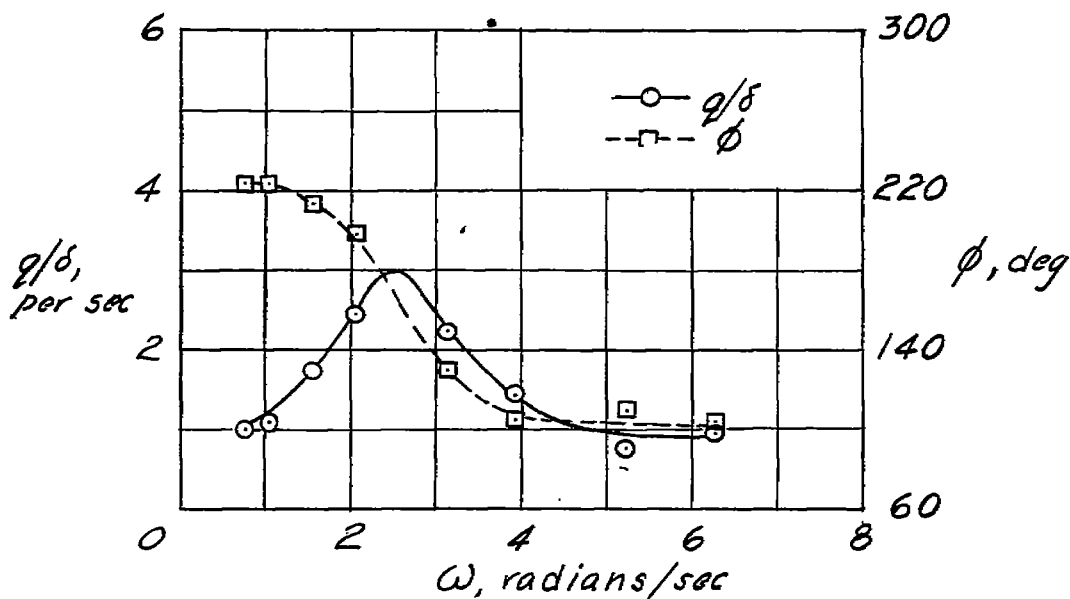
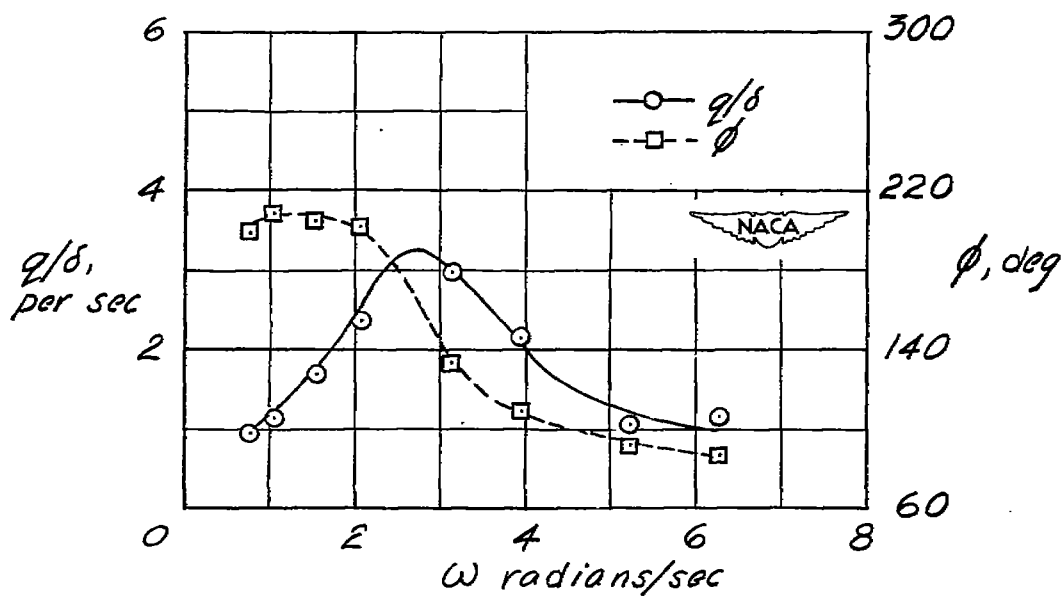
(c) $M = 0.72$; $h_p = 30,000$ feet; $i_t = 2.1^\circ$.(d) $M = 0.75$; $h_p = 29,000$ feet; $i_t = 2.1^\circ$.

Figure 5.- Continued.

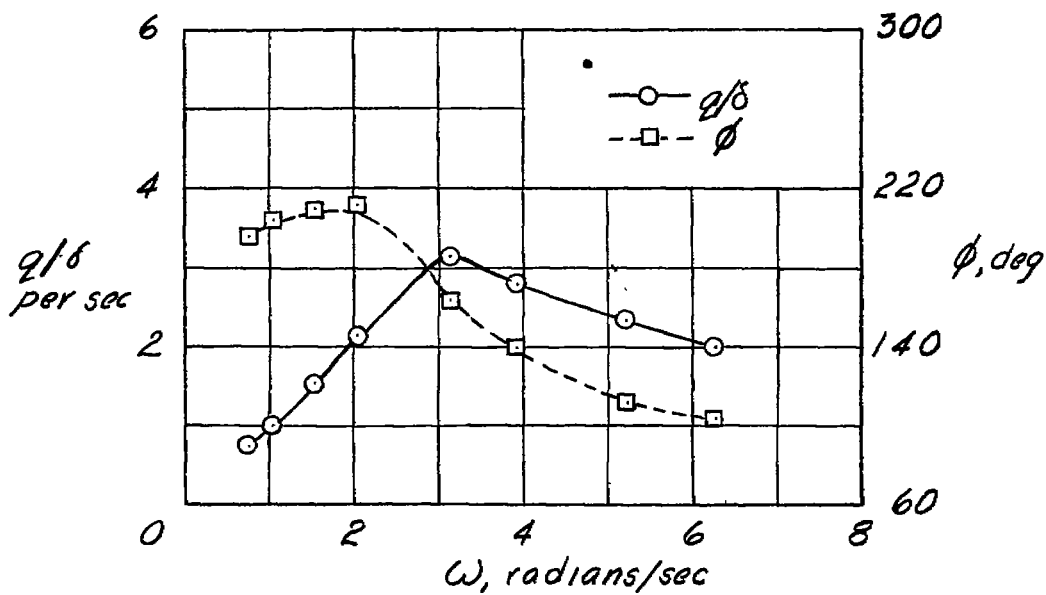
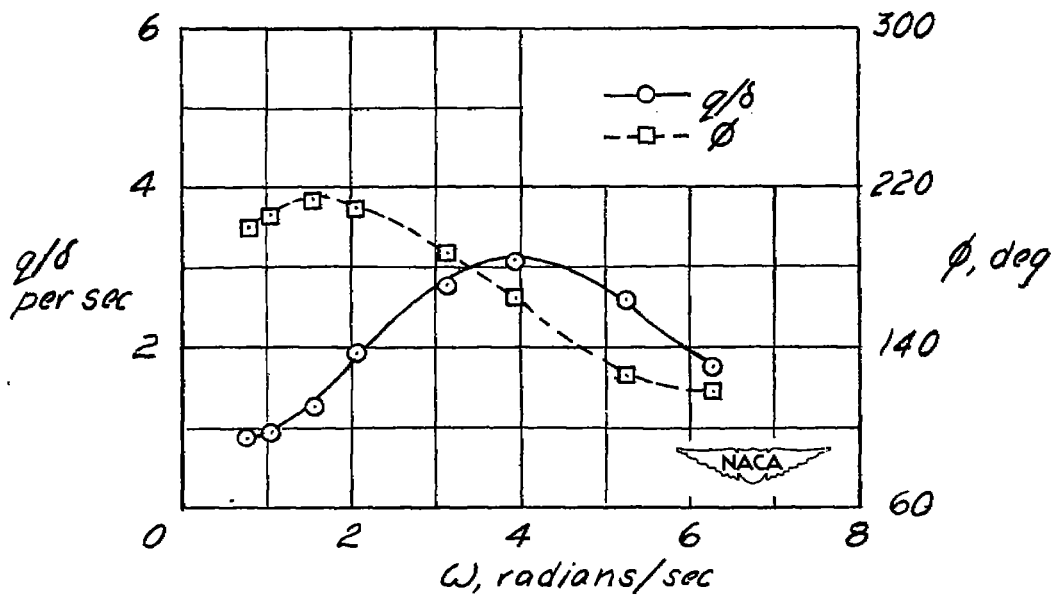
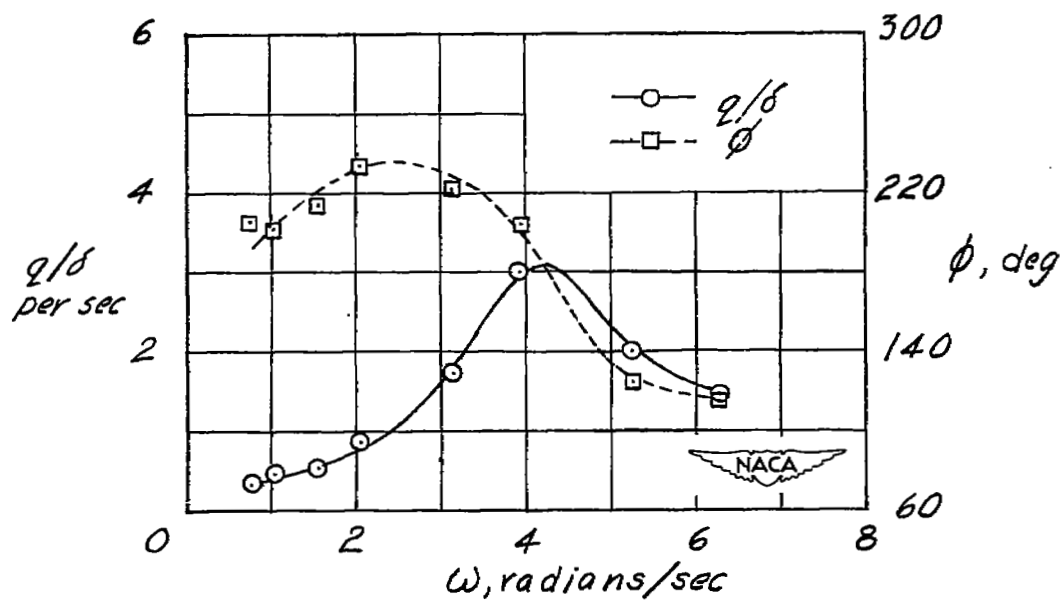
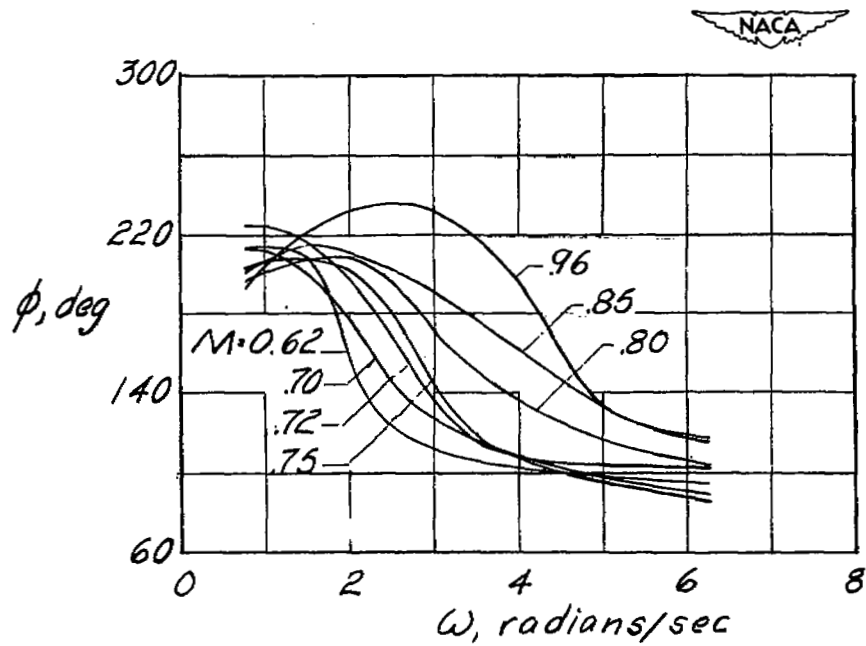
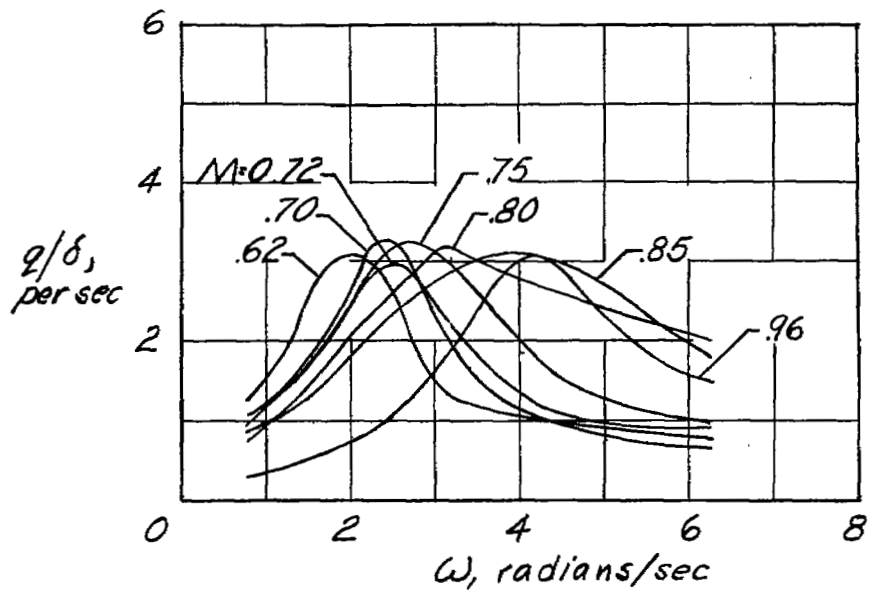
(e) $M = 0.80$; $h_p = 28,000$ feet; $i_t = 2.1^\circ$.(f) $M = 0.85$; $h_p = 29,000$ feet; $i_t = 1.3^\circ$.

Figure 5.- Continued.



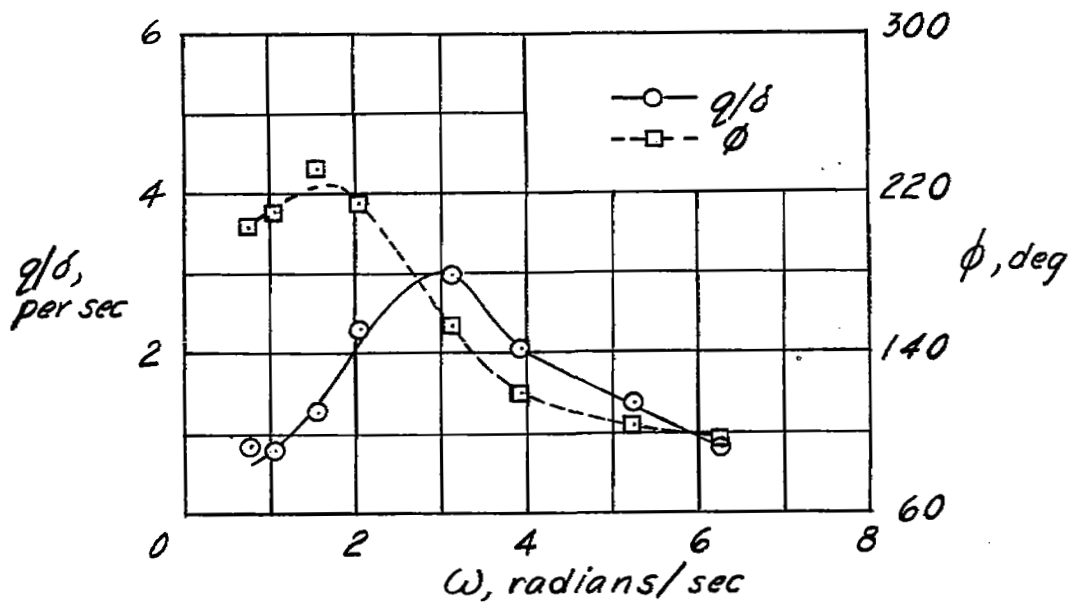
(g) $M = 0.96$; $h_p = 33,000$ feet; $i_t = 1.6^\circ$.

Figure 5.- Continued.

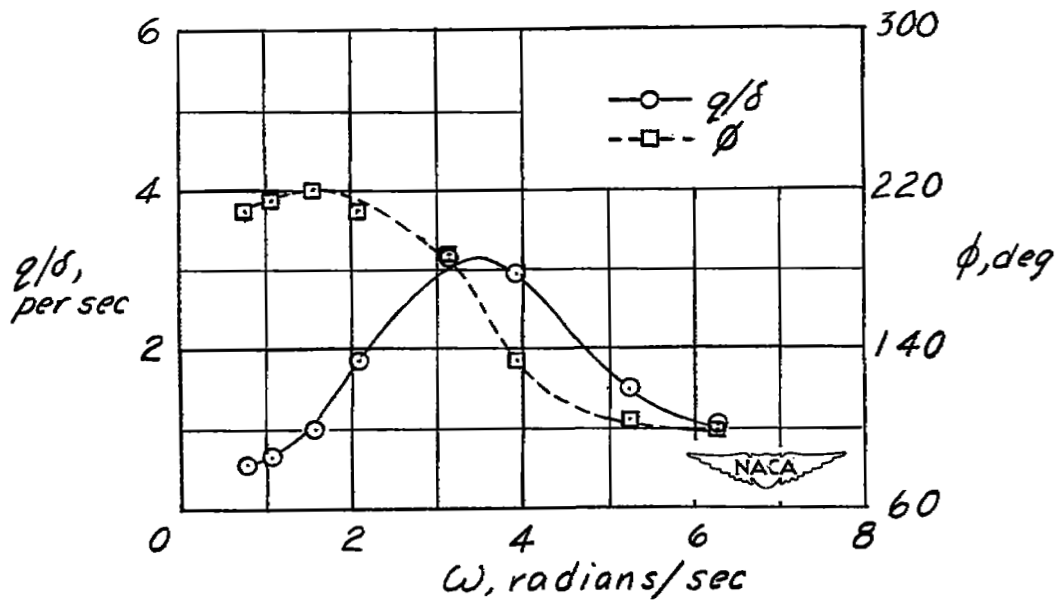


(h) $h_p = 28,000$ to $33,000$ feet.

Figure 5.- Concluded.

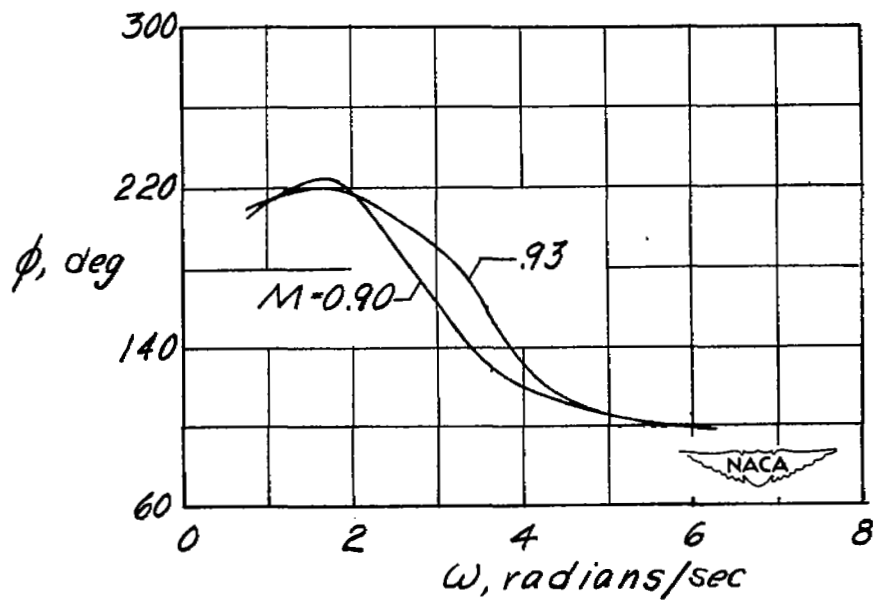
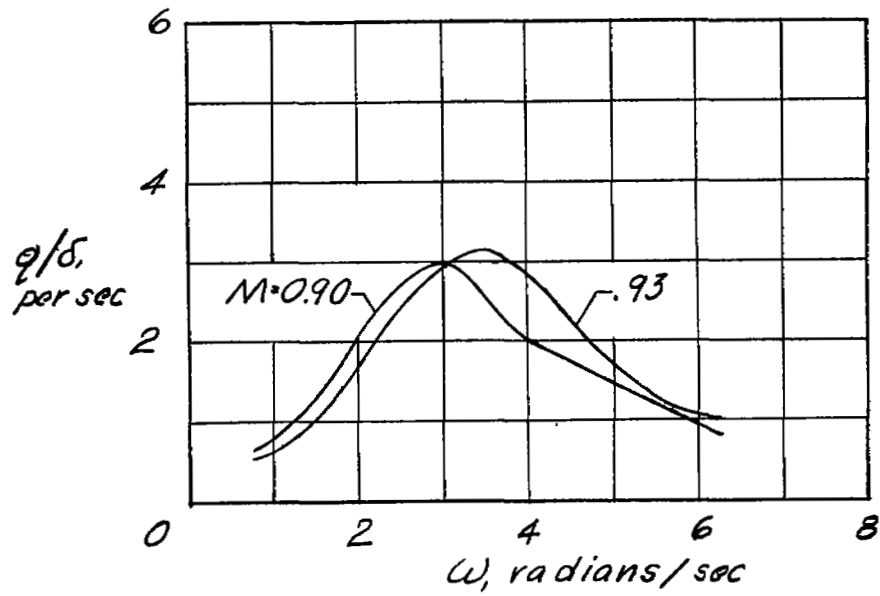


(a) $M = 0.90$; $h_p = 43,000$ feet; $i_t = 1.0^\circ$.



(b) $M = 0.93$; $h_p = 37,500$ feet; $i_t = 2.4^\circ$.

Figure 6.- Frequency response of the Douglas D-558-II airplane at 37,500 and 43,000 feet.



(c) $h_p = 43,000$ and $37,500$ feet.

Figure 6.- Concluded.

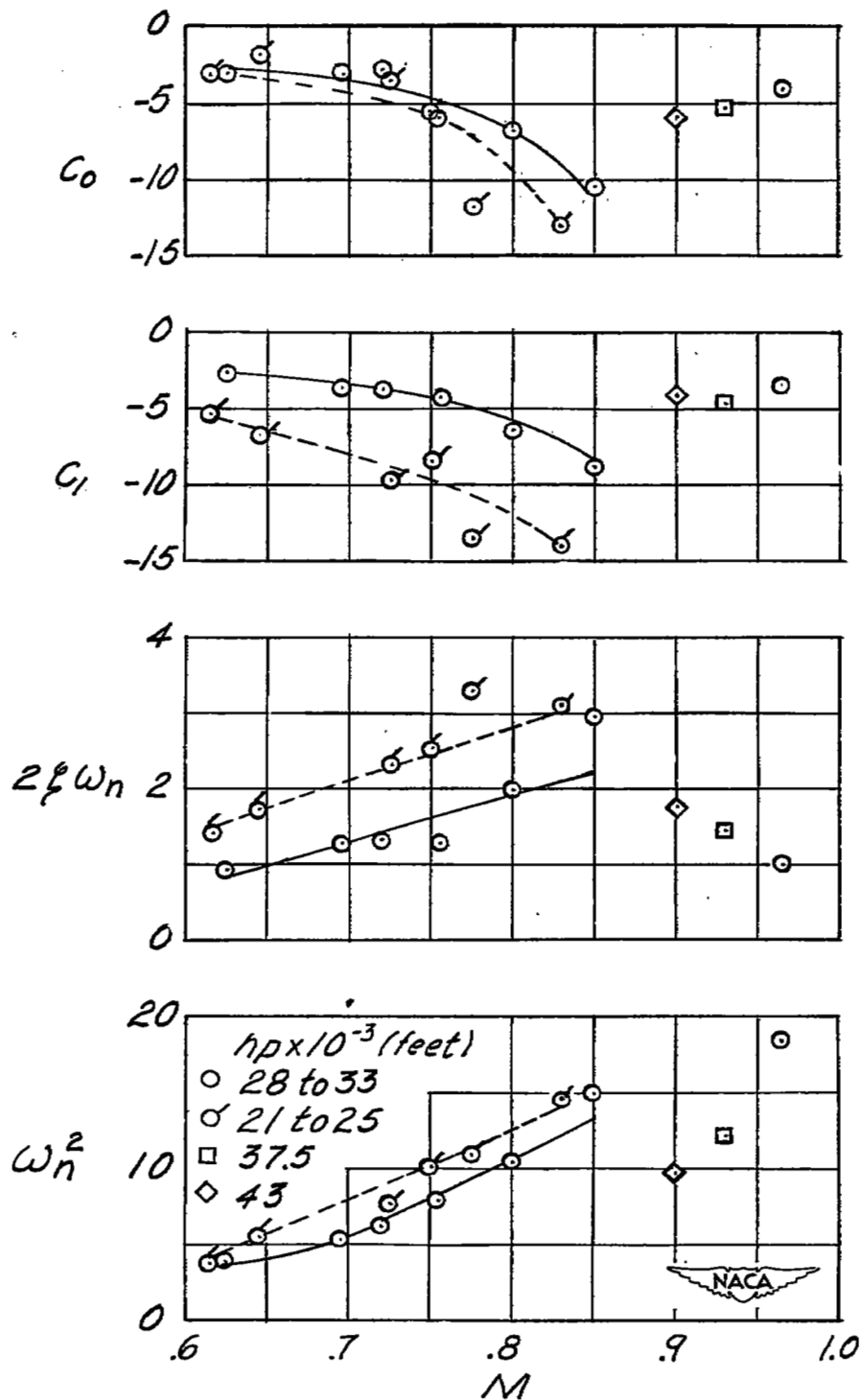


Figure 7.- Variation of airplane transfer-function coefficients with Mach number.

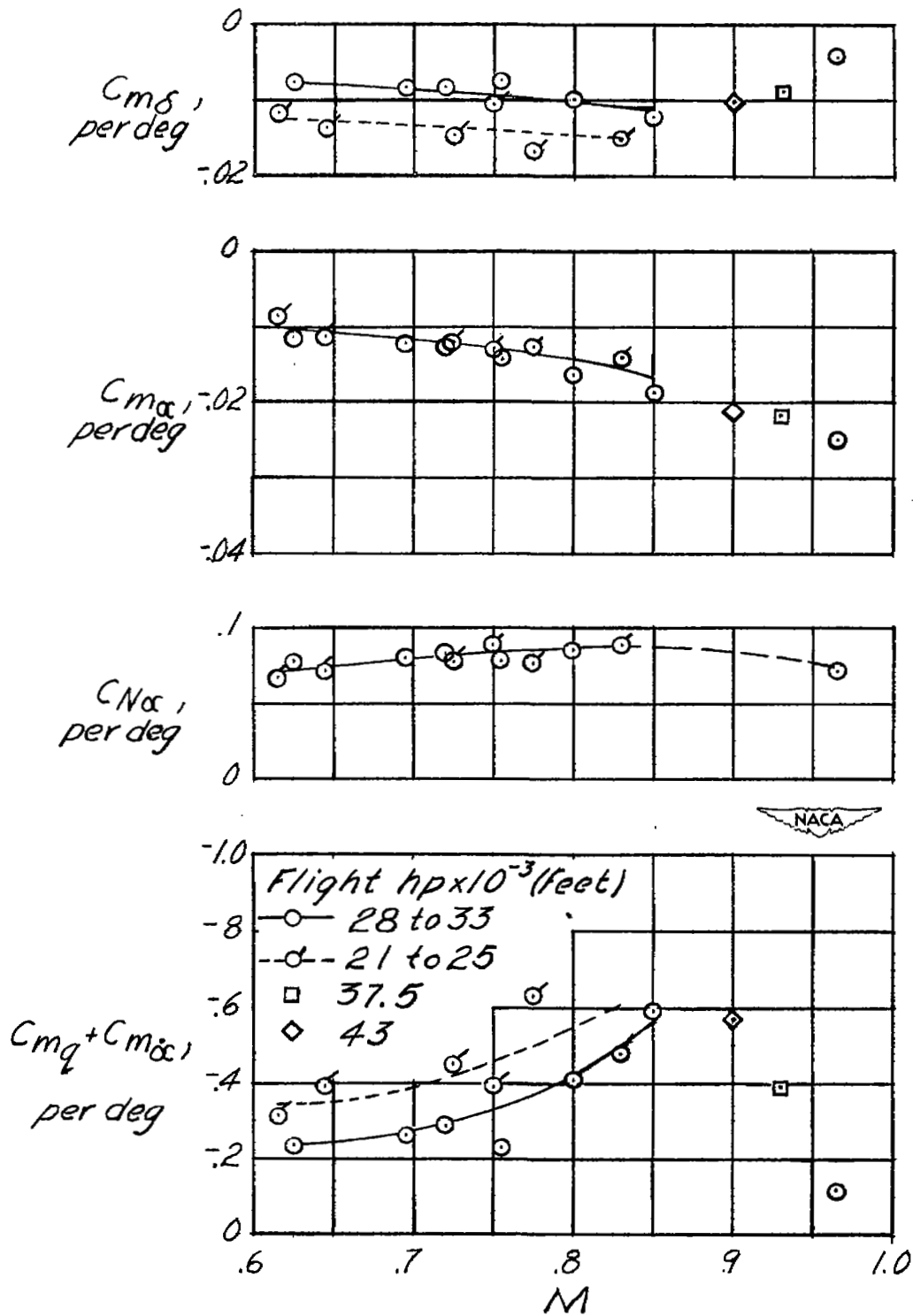


Figure 8.- Variation of the airplane stability derivatives with Mach number.

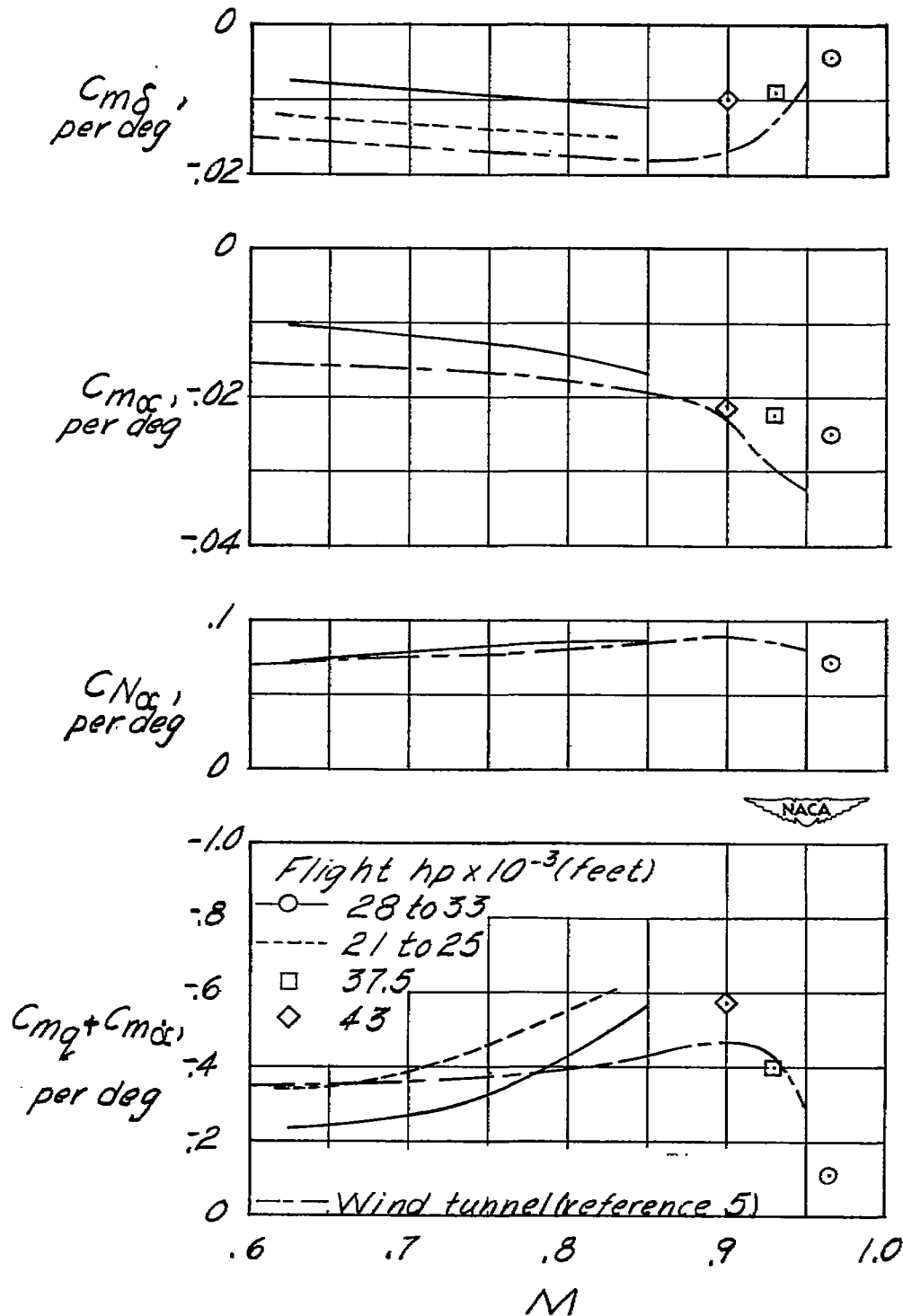


Figure 9.- Comparison of the airplane stability derivatives with those calculated from wind-tunnel results.

SECURITY INFORMATION

NASA Technical Library



3 1176 01436 4674

